Gap solitons in $\mathcal{PT}$-symmetric lattices with a lower refractive-index core

Liangwei Dong,[1,*] Linlin Gu,[2] and Dengchu Guo[2]
[1]*Institute of Information Optics, Zhejiang Normal University, Jinhua 321004, China*
[2]*Department of Physics, Zhejiang Normal University, Jinhua 321004, China*
(Received 9 December 2014; published 15 May 2015)

We address the existence and stability properties of families of gap solitons in a lower refractive-index core, sandwiched between two optical lattices with a parity-time ($\mathcal{PT}$) symmetry imprinted in a defocusing medium. The scale of flat-topped complex solitons can be controlled arbitrarily by varying the embedded index core. Multipeaked solitons are found to exhibit equal peak values in the region of the index core, and they have no analog in other lattice-modulated or bulk media. We demonstrate that, in sharp contrast to solitons in regular $\mathcal{PT}$ lattices, flat-topped and multipeaked solitons are either stable or suffer a negligibly weak instability, even when the gain-loss coefficient approaches the $\mathcal{PT}$-symmetry-breaking point. Our results, thus, build a bridge between the $\mathcal{PT}$ defect solitons in a narrow index core and the $\mathcal{PT}$ kink pairs in a broad index core. We also suggest an effective way for the observation of "surface solitons" in $\mathcal{PT}$-symmetric lattices.

DOI: 10.1103/PhysRevA.91.053827 PACS number(s): 42.65.Tg, 42.65.Jx, 42.65.Wi

I. INTRODUCTION

The interplay between nonlinearity, periodicity of the underlying structure, and local lattice deformations has attracted broad attention during the past decade, since it offers new possibilities for the realization of different types of spatial solitons. For a review of early works, see, e.g., [1] and references therein. The appropriate modulation of these freedoms can be utilized to suppress the instability of solitons, which is crucial for their applications in practice.

The dynamics of solitons in nonlinear media modulated by complex lattices exhibiting a $\mathcal{PT}$ symmetry has been a topic of continuously renewed interest recently, due to their fundamental physics and potential applications in various physical fields [2–4]. $\mathcal{PT}$ symmetry demands that a Hamiltonian share a common eigenfunction set with the $\mathcal{PT}$ operator. The parity operator $\widehat{P}$, responsible for spatial reflection, is defined through the operations $\widehat{p} \to -\widehat{p}$, $\widehat{x} \to -\widehat{x}$, whereas the time-reversal operator $\widehat{T}$ leads to $\widehat{p} \to -\widehat{p}$, $\widehat{x} \to \widehat{x}$, and $\widehat{i} \to -\widehat{i}$. From the normalized Schrödinger equation $i\Psi_t = \widehat{H}\Psi$ [$\widehat{H} = \widehat{p}^2/2 + V(x)$ and $\widehat{p} = -i\frac{\partial}{\partial x}$], one can deduce that $\widehat{T}\widehat{H} = \widehat{p}^2/2 + V^*(x)$, which results in $\widehat{H}\widehat{P}\widehat{T} = \widehat{p}^2/2 + V(x)$ and $\widehat{P}\widehat{T}\widehat{H} = \widehat{p}^2/2 + V^*(-x)$. Thus, a necessary condition for the Hamiltonian to be $\mathcal{PT}$ symmetric is that the potential function $V(x)$ should satisfy the condition $V(x) = V^*(-x)$ [5–7]. The importance of a $\mathcal{PT}$ symmetry lies in that a non-Hermitian Hamiltonian can display entirely real spectra [2–7]. Diverse families of spatial solitons were explored theoretically and observed experimentally in $\mathcal{PT}$-symmetric potentials with gain-loss components [8–20].

On the other hand, series of fascinating applications have been revealed in photonic crystal fibers (PCFs) with a high-contrast refractive-index modulation [21,22]. An analog of a PCF-like structure with a low-contrast modulation was reported in nonlinear systems as well [23]. The latter case is similar to the optically induced real lattices with a defect, in which stable nonlinear defect states may exist [24]. In real lattices with an index core, localized stable flat-topped and dipole solitons were found [25]. The reverse setting, i.e., an optical lattice with a finite number of sites, can support symmetric and antisymmetric solitons with a nonvanishing intensity at infinity [26]. In the two-dimensional case, soliton shape can be controlled by varying the shape of the lattice defects [27].

We should note that all works on defect solitons in $\mathcal{PT}$ lattices focused on a defect covering a single lattice site [11,12,28]. Moreover, to our knowledge, solitons in lattices with gain-loss defects have not yet been reported elsewhere. As is well known, the dynamics of solitons in $\mathcal{PT}$ lattices is dramatically different from that of solitons in real lattices [8–20], especially when the gain and loss are strong. Considering the fact that flat-topped and dipole solitons can exist in an index core embedded in a real lattice, it is natural to ask: Can solitons can be supported by a defect covering several $\mathcal{PT}$ lattice sites? If yes, what is their dynamics and how do the low-index core and the gain-loss components influence them?

To answer these questions, we investigate the properties of spatial solitons in a low-refractive-index core, surrounded by two optical lattice walls with a $\mathcal{PT}$ symmetry. By analogy with solid-state physics, localized nonlinear modes with well-defined borders and abruptly decaying wings can be termed as domain solitons [25]. Flat-topped solitons with arbitrary scale can be derived by varying the size of the index core. The influence of the gain-loss component on the stability of solitons is studied in detail. Particularly, we find a class of multipeaked solitons with equal peak value, which have no analog in real lattices and are different from the multipeaked solitons in regular $\mathcal{PT}$ lattices [29]. The confinement of lattice walls and the Bragg reflections on beams suppress the instability of solitons remarkably. Unstable solitons are very robust and can propagate for a long distance (thousands of diffraction lengths) with no obvious distortion.

II. THEORETICAL MODEL

We consider light propagation along the z axis in a defocusing Kerr medium with a transverse complex refractive-index modulation. The dynamics of the beam can be described by the dimensionless nonlinear Schrödinger

*donglw@zjnu.cn

equation [30,31]

$$i\frac{\partial A}{\partial z} = -\frac{1}{2}\frac{\partial^2 A}{\partial x^2} + |A|^2 A - p[V(x) + ip_i W(x)]A, \quad (1)$$

where A is the complex field amplitude; x and z are the normalized transverse and longitudinal coordinates, respectively; p is the depth of lattice; and $V(x)$ and $W(x)$ correspond to the distribution of the real and imaginary refractive-index modulation. To study the domain solitons in a low-refractive-index core, we set $V(x) = \cos^2(\Omega x)$, $W(x) = \sin(2\Omega x)$ for $|x| \geqslant n\pi/2\Omega$ and $V(x) = 0$ and $W(x) = 0$ otherwise. Here Ω denotes the frequency of the lattice and n is the number of lattice periods removed from the $\mathcal{PT}$ lattice to form a low-index core. Obviously, $V(x)$ and $W(x)$ satisfy the demand of $\mathcal{PT}$ symmetry; i.e., $V(-x) = V(x)$, $W(-x) = -W(x)$. Here $p_i \in [0,0.5]$ characterizes the relative strength of gain and loss. The $\mathcal{PT}$ lattice degenerates to a purely real harmonic lattice when $p_i = 0$ and reaches a symmetry-breaking point if $p_i = 0.5$, beyond which the system undergoes an abrupt phase transition. In particular, above this critical threshold, the system loses its $\mathcal{PT}$ property and as a result some of the eigenvalues become complex [5]. For a typical input beam with $\lambda = 1$ μm, $a = 10$ μm (beam width) and $n_0 = 3$, $x = 1$ and $z = 1$ in the dimensionless Eq. (1) correspond to $\sim 10\,\mu$m in the transverse direction and ~ 7 mm in the propagation direction. Here $p = 1$ corresponds to a maximum variation of refractive index $\sim 8 \times 10^{-5}$.

We plot an example of a sandwiched $\mathcal{PT}$ lattice with a low-index core in Fig. 1(a). The two lattices surrounding the index core form a well, which can be utilized to capture the nonlinear bound states. Before we discuss the properties of solitons, it is important to understand the Floquet-Bloch spectrum of a periodic lattice without an index core. Although the soliton mainly resides in the core region, the oscillatory tails or wings of the nonlinear mode unavoidably penetrate into the bulk of lattice. Thus, the existence region of solitons is still restricted in the gaps of the $\mathcal{PT}$ lattice. To solve the band-gap lattice spectrum, we search for solutions of the linear version of Eq. (1) in the form $A(x,z) = q(x)\exp(ikx + ibz)$, where k is the transverse Bloch wave number, b is the longitudinal wave number, and $q(x) = q(x + 2\pi/\Omega)$ is the complex periodic function [32]. Substitution of it into Eq. (1) yields the eigenvalue problem

$$bq = \frac{1}{2}\left(\frac{\partial^2 q}{\partial x^2} + 2ik\frac{\partial q}{\partial x} - k^2 q\right) + p[V(x) + ip_i W(x)]q, \quad (2)$$

which can be solved numerically by the plane-wave expansion method [33].

Note that the generalization of the Bloch theorem into a system with complex periodic potentials is valid only when the following two conditions are satisfied. First, the periodicity of the real part of the potential is equal to that of the imaginary part. In this case, both parts of the complex potential can be decomposed to a Fourier series with the same frequency ($n\Omega, n = 0, \pm 1, \pm 2,$). The appearance of gain and loss results in an asymmetry of coefficients in addition to the fundamental Fourier component ($n = 0$), which are symmetric for a system with real periodic potentials. Second, the imaginary part of the potential is odd symmetric. This property guarantees that the opposite gain and loss components in each lattice periodicity compensate each other, which eliminates the imaginary coefficients before all Fourier components.

The band-gap structure of a lattice with $p_i = 0.1$ is shown in Fig. 1(b). It consists of a single semi-infinite gap and an infinite number of finite gaps expanding with the growth of lattice depth p. In the following discussions, we focus our attention on solitons residing in the first finite gap, because in defocusing media, solitons can only be found in finite band gaps. The detail of a lattice spectrum at $p = 4$ is illustrated in Fig. 1(c). The open gaps shrink with the growth of p_i and are entirely closed at the symmetry-breaking point $p_i = 0.5$, after which the gain-loss component plays a dominant role and the lattice spectrum becomes partly complex [Fig. 1(d)].

We search for stationary solutions of Eq. (1) by assuming $A(x,z) = q(x)\exp(ibz)$, where q is complex and represents the profile of the light field; b stands for a propagation constant. Substitution of the above expression into Eq. (1) yields the following nonlinear ordinary differential equation:

$$\frac{1}{2}\frac{d^2 q}{dx^2} - bq + p[V(x) + ip_i W(x)]q - |q|^2 q = 0, \quad (3)$$

from which, by applying the boundary conditions $q_{r,i}(x \to \pm\infty) = 0$, the stationary solution can be solved numerically either by the Newton iterative method or by the squared operator iteration method [34].

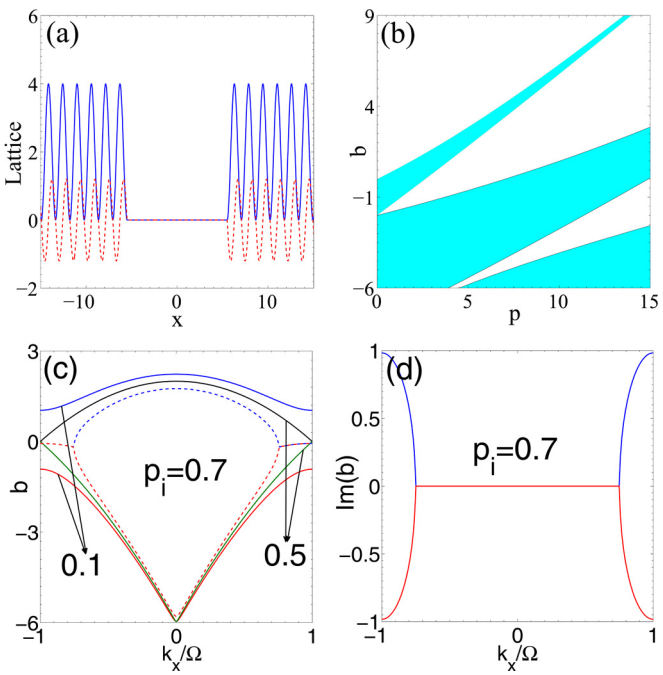

FIG. 1. (Color online) (a) Profile of defected $\mathcal{PT}$ lattice with $p = 4$, $p_i = 0.1$, and $n = 7$. Solid blue line, real part; dashed red line, imaginary part. (b) Band-gap lattice spectrum versus lattice depth p at $p_i = 0.1$. (c) Band-gap structure of the lattice at $p = 4$. Dashed line indicates the real eigenvalues of b at $p_i = 0.7$. (d) Imaginary part of the double-valued band at $p_i = 0.7$. $\Omega = 2$ hereinafter. All quantities are plotted in dimensionless units.

To study the stability of solitons in a system described by the nonlinear Schrödinger equation, one can consider the eigenvalues of small perturbations on the stationary solutions in the form $A(x,z) = \{q(x) + [v(x) - w(x)]\exp(\lambda z) + [v(x) + w(x)]^* \exp(\lambda^* z)\}\exp(ibz)$, where q is the stationary solution solved from Eq. (3); $v, w \ll 1$ are the infinitesimal perturbations, and the superscript $*$ denotes the complex conjugation. Substituting the perturbed solution into Eq. (1) and linearizing it around q leads to coupled linear equations of an eigenvalue problem [31]:

$$\lambda \begin{bmatrix} v \\ w \end{bmatrix} = -i \begin{bmatrix} i\mathrm{Im}(q^2) - ipp_i W & \widehat{L} + \mathrm{Re}(q^2) \\ \widehat{L} - \mathrm{Re}(q^2) & -i\mathrm{Im}(q^2) - ipp_i W \end{bmatrix} \begin{bmatrix} v \\ w \end{bmatrix}. \tag{4}$$

Here, $\widehat{L} = \frac{1}{2}\frac{d^2}{dx^2} - b + pV - 2|q|^2$. Equations (4) can be solved numerically by a finite-difference method. The stability of a soliton is determined by the spectrum of the above linearization operator. Solitons can propagate stably only when all real parts of eigenvalue λ equal zero.

III. FLAT-TOPPED GAP SOLITONS

First, we discuss the properties of flat-topped gap solitons in lattices with different sizes of index cores and a relatively weak gain-loss component ($p_i = 0.1$). The dependence of power [defined as $P = \int_{-\infty}^{\infty} |q(x)|^2 dx$] on propagation constant b for solitons in lattices with different n is shown in Fig. 2(a). It decreases monotonically with b and varnishes when b exceeds an upper cutoff of propagation constant b_{upp} or is below a lower cutoff b_{low}. At fixed b, the power increases with the growth of index core size n.

Two typical examples of soliton profiles in lattices with different n are displayed in Figs. 2(b) and 2(c). While the oscillatory tails or wings of nonlinear modes penetrate into the bulk of the lattices, solitons are mainly confined in the low-index core region between the two lattice walls. The delocalization length and peak amplitude decrease with the growth of b. When the core region is wide and b is small, the modulus of the soliton exhibits a flat-topped shape [Fig. 2(b)]. The height of the flat top of the soliton at $b = -0.6$ in Fig. 2(b) is 0.7746, which is just equal to $\sqrt{|-0.6|}$. By assuming n is very large, it follows from Eq. (3) that $|q(x \to \pm\infty)| = \sqrt{-b}$, which means that gap solitons can be found only at $b < 0$, in contrast to localized gap surface solitons requiring $b > 0$ [32]. Thus, flat-topped gap solitons can be intuitively regarded as a pair of symmetric kink solitons or shock waves with pedestal height equaling $\sqrt{|b|}$ and abruptly decaying tails in the lattice sites [35]. If the core region is narrow, the distribution of the soliton modulus is similar to the defect solitons reported in [12]. The PCF-like structure with a low-index core, therefore, bridges a gap between the surface kink pairs and the defect solitons in complex lattices with a $\mathcal{PT}$ symmetry.

Due to the demand of $\mathcal{PT}$ symmetry, in complex lattices, one cannot find the analog of surface solitons at the edge of a real semi-infinite lattice. However, the kink solitons at an edge of a lattice can be obviously classified as surface solitons [35]. Consequently, we propose a simple model for the realization of symmetric surface solitons in $\mathcal{PT}$ lattices, which may be useful in their practical applications, e.g., for exploring the optical properties at the interface separating a low-index core and a semi-infinite lattice with gain and loss.

In $\mathcal{PT}$ lattices, the nontrivial phase distribution of complex nonlinear modes leads to the arising of power-flow density in the form $S = (i/2)(qq_x^* - q_x^* q)$ [2]. The power-flow density

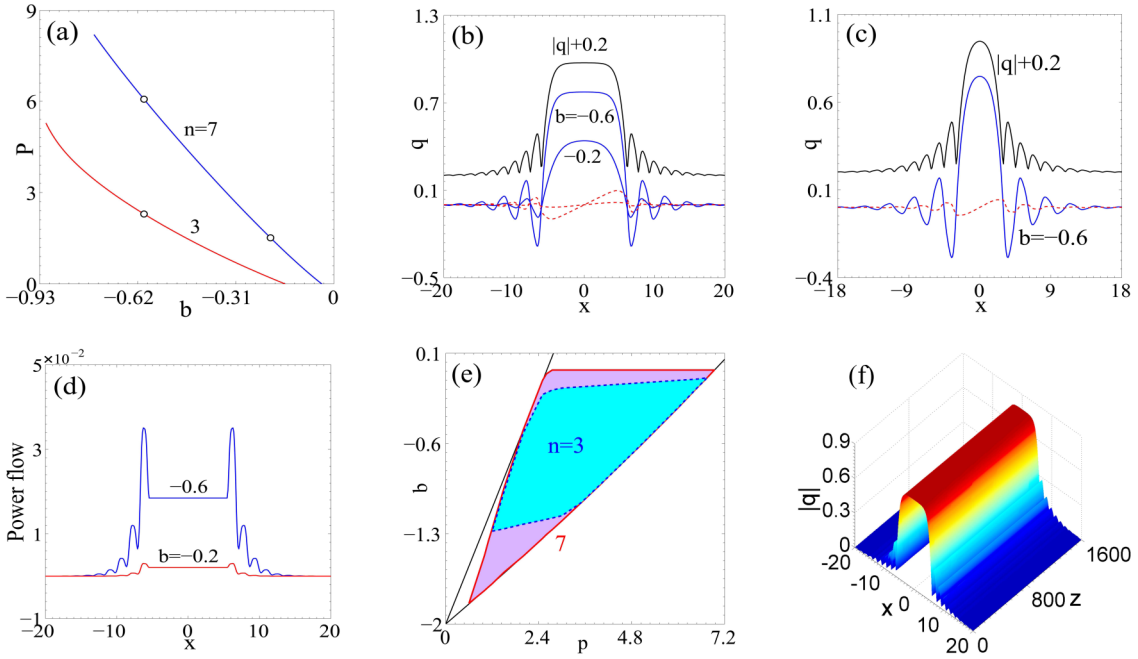

FIG. 2. (Color online) (a) Power P versus propagation constant b for solitons in lattices with different n. (b, c) Profiles of solitons marked in (a) in lattices with $n = 7$ and 3. (d) Transverse power flow of solitons shown in (b) across the lattice. (e) Existence regions of solitons at the p,b plane for $n = 7$ (solid line) and 3 (dashed line). (f) Propagation simulation of a soliton at $b = -0.6$ shown in (b). The modulus of the soliton is displayed. $p = 4$ except for (e), and $p_i = 0.1$ in all panels. All quantities are plotted in dimensionless units.

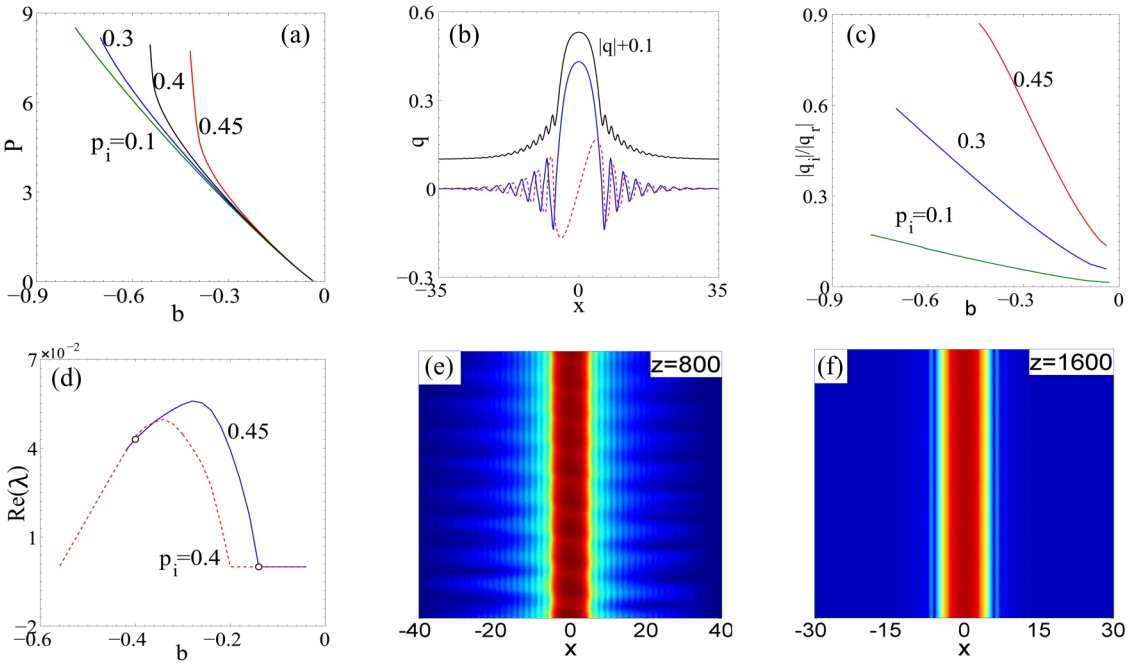

FIG. 3. (Color online) (a) Power P versus propagation constant b for solitons at different p_i. (b) Profile of soliton at $b = -0.2$, $p_i = 0.45$. (c) Amplitude ratio of the imaginary and real parts of solitons versus b. (d) Instability growth rate versus b. (e) Unstable and (f) stable propagation of solitons marked by circles in (d). The modulus of solitons is displayed; $p = 4$, $n = 7$ in all panels. All quantities are plotted in dimensionless units.

corresponding to solitons shown in Fig. 2(b) is plotted in Fig. 2(d). $S > 0$ everywhere implies that the power always flows in one direction, i.e., from the gain toward the loss region. Intriguingly, S remains a constant value in the region of the index core and varies symmetrically in the near-interface lattice sites.

The existence regions of gap solitons in lattices with varying p and different n are shown in Fig. 2(e). We make five comments here. First, solitons can only be found in the open gap of $\mathcal{PT}$ lattices. Second, solitons stop to exist either when the lattice is too deep ($p > p_{\rm upp}$) or when the lattice is too shallow ($p < p_{\rm low}$). Third, the existence region shrinks with the decrease of n. One can expect that the existence region will occupy the whole gap (with a constant upper cutoff) when n is big enough. Fourth, in a lattice with $n = 7$, $b_{\rm upp}$ is a constant for $p \geqslant 2.75$ and is a linearly decreasing function of p if $p \leqslant 2.62$. Fifth, at larger n, while $b_{\rm low}$ always coincides with the lower edge of the first gap, $b_{\rm upp}$ partially coincides with the upper gap edge ($p \in [1.92, 2.62]$). If the index core is narrow, $b_{\rm low}$ partially coincides with the lower gap edge when p exceeds a critical value, e.g., $p_{\rm cr} = 3.36$ at $n = 3$.

To explore the stability properties, based on Eqs. (4), we perform a linear stability analysis on the stationary solutions mentioned above and find that gap solitons are completely stable in their entire existence regions provided that the gain-loss coefficient p_i is relatively small. To test the predictions of linear-stability analysis, we solve Eq. (1) numerically by the standard beam-propagation method, and a representative propagation example is illustrated in Fig. 2(f). It manifests the strong guiding ability of a PCF-like structure, even though the odd-symmetric gain and loss are added into the lattice.

Next, we address the influence of the gain-loss component of the $\mathcal{PT}$ lattice on the existence and stability of gap solitons. The lower cutoff $b_{\rm low}$ decreases with the growth of p_i [Fig. 3(a)], because the lower gap edge shown in Fig. 1(b) increases with p_i and coincides with the descending upper edge when $p_i = 0.5$. In other words, the shrinkage of the first finite gap with the growth of p_i narrows the existence region of solitons. The nature of defocusing nonlinearity results in all power curves of solitons at different p_i being monotonic functions on b. In comparison with the profiles of solitons in a lattice with weak gain and loss [Fig. 2(b)], it is immediately found that the imaginary part of the soliton is enhanced in the lattice with larger p_i [Fig. 3(b)].

The ratios between the maxima of imaginary and real parts of solitons are plotted in Fig. 3(c). The peak of the imaginary part increases with the decrease of b. It becomes more obvious when the gain-loss parameter p_i is large. Interestingly, the radio at $b_{\rm low}$ approximately equals twice the ratio between the coefficients before the real and imaginary lattice components. Note that the real index modulation $\cos^2(\Omega x)$ can be rewritten as $[1 + \cos(2\Omega x)]/2$, which implies that the coefficient p_r before the $\cos^2(\Omega x)$ is actually $1/2$. It leads to the ratio between the imaginary and real lattice components being limited in the scope of $[0,1]$. For example, the ratio between $\max|q_i|$ and $\max|q_r|$ at $p_i = 0.3$ is 0.6, which is justly equal to $p_i/p_r = 0.3/0.5$. The physical explanation may be attributed to the fact that the modulation of the linear refractive index plays a main role in the distribution of solitons when b approaches the lower gap edge of the $\mathcal{PT}$ lattice. One can also infer from Fig. 3(c) that the upper cutoffs are independent of the strength of the gain-loss parameter p_i. All solitons cease to exist at the same value $b_{\rm upp} = -0.03$. It is in good agreement with the existence condition of surface kink solitons, i.e., $b < 0$.

The results of the linear stability analysis on solitons in lattices with different p_i are summarized in Fig. 3(d). Although

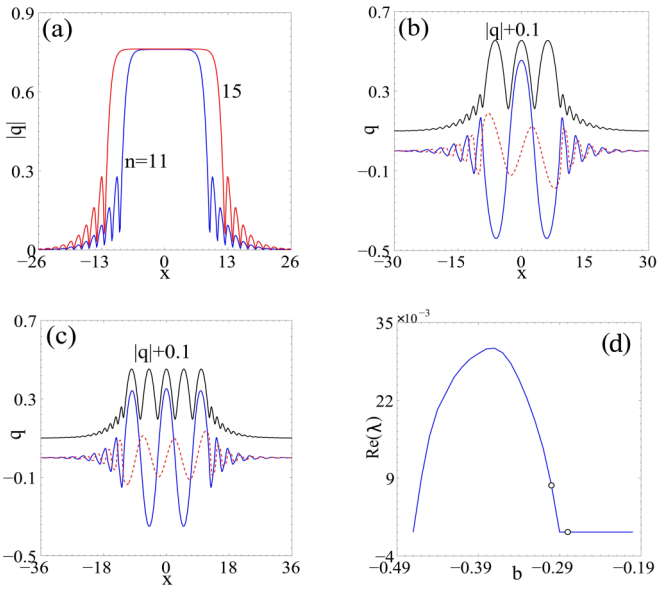

FIG. 4. (Color online) (a) Moduli of flat-topped solitons at $b = -0.58$ in lattices $p_i = 0.1$. (b) Profile of three-peaked solitons at $b = -0.3$ ($p_i = 0.4$, $n = 11$), (c) profile of five-peaked solitons at $b = -0.3$ ($p_i = 0.4$, $n = 15$), and (d) instability growth rate versus propagation constant b ($p_i = 0.4$, $n = 15$). $p = 4$ in all panels. All quantities are plotted in dimensionless units.

an oscillatory instability arises for solitons with high power or small b, it is very weak ($\sim 1 \times 10^{-3}$) and the distortion of solitons due to the instability can almost be ignored. As p_i approaches the symmetry-breaking point, solitons are still very robust. This is in sharp contrast to the stability of solitons in regular or single-site defected $\mathcal{PT}$ lattices, where the large p_i unavoidably destroys the solitons after a short propagation distance. Instances of unstable and stable propagation of solitons are presented in Figs. 3(e) and 3(f), respectively. They manifest again the strong ability of PCF-like structures for trapping and guiding beams, even when the gain and loss are very strong.

IV. MULTIPEAKED GAP SOLITONS

The moduli of flat-topped solitons in lattices with larger index cores are displayed in Fig. 4(a). By comparison with the side lobes in the lattice sites, one finds that the moduli of two solitons are almost identical, except for their spatial sizes. It can be easily understood if we treat the solitons as a kink pair. Recalling the solitons shown in Fig. 2(b), we find that the scale of flat-topped solitons can be controlled arbitrarily by varying the size of the embedded index core. The height of the flat top is still equal to the square root of $|b|$, provided that the power of the solitons exceeds a certain value or b is small.

We should note that multipole solitons with out-of-phase neighboring components and multipeaked solitons with in-phase neighboring components were widely reported in diverse nonlinear schemes. However, higher-order solitons with a same peak value for each pole or hump were rarely reported, with only few exceptions, e.g., truncated-Bloch-wave solitons in real lattices [36], truncated-Bloch-wave solitons in $\mathcal{PT}$ lattices [29], and multistable solitons in $\mathcal{PT}$ lattices imprinted in competing cubic-quintic media [37]. The equal peaks of the above solitons reside in the neighboring successive lattice channels. In the following discussions, we elucidate a class of solitons with several peaks in the core region of a $\mathcal{PT}$ lattice. Unlike the solitons in [29,36,37], there are no lattice channels for guiding the soliton poles.

Similar to the flat-topped solitons in Sec. III or solitons in regular $\mathcal{PT}$ lattices, the real and imaginary parts of multipeaked solitons are also even and odd symmetric [Figs. 4(b) and 4(c)], respectively, which is consistent with the symmetry of lattices. The three-peaked soliton is composed of a tripole real part and a quadrupole imaginary part. The five-peaked soliton is a combination of a real part with five poles and an imaginary part with six poles. However, the modulus or intensity of the beam exhibits a multipeaked structure, in which all main peaks are of the same value. It may be explained in physics that the optical material always feels the intensity of the beam, no matter how the real and imaginary parts of the beam are distributes. Once the interplay between the refractive index of the material and the intensity of the light beam stops, the beam develops into an eigenmode of a nonlinear system and a soliton forms. The superposition of out-of-phase fundamental solitons at different positions constructs a bounded nonlinear state in the present scheme. The multipeaked solitons may also be understood by analogy with the formation mechanism of standing waves in other fields of physics. A soliton with more peaks can be found if one enlarges the size of the index core.

The linear stability analysis results shown in Fig. 4(d) are in good agreement with the direction numerical propagation simulations [Figs. 5(a) and 5(b)]. Unstable solitons still

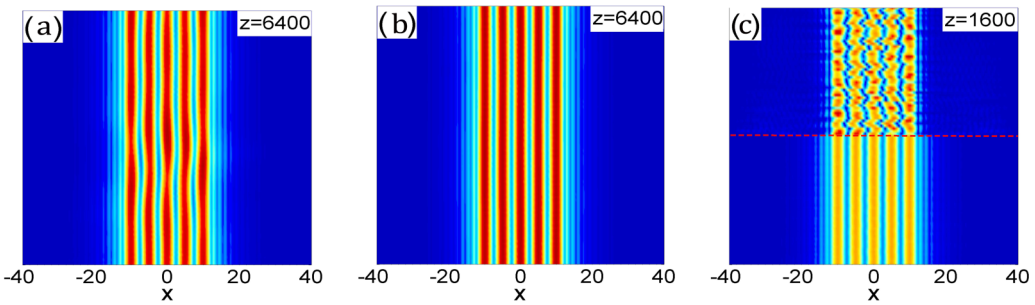

FIG. 5. (Color online) (a) Unstable and (b) stable propagations of five-peaked solitons marked by circles in Fig. 4(d). (c) Propagation of a five-peaked soliton at $b = -0.28$. The gain-loss component of the lattice is removed at $z = 800$. All quantities are plotted in dimensionless units.

propagate robustly for a very long distance (thousands of diffraction lengths) without obvious distortions, greatly exceeding the present experimentally feasible sample lengths, even in a lattice with strong gain and loss. To further illustrate that the gain-loss component of the lattice is necessary for the stable propagation of a soliton, we remove the imaginary part of the lattice at a certain propagation distance and the simulation result is shown in Fig. 5(c). The stable propagation becomes a wild disorder though the main energy of the soliton is still confined in the index core region.

V. CONCLUSIONS

To summarize, we report on the dynamics of spatial gap solitons in a defocusing Kerr medium with an imprinted $\mathcal{PT}$-symmetric lattice, whose core region is replaced by a defect covering several lattice sites. Such a sandwiched PCF-like complex structure can be utilized to guide different families of stable localized nonlinear states, i.e., flat-topped solitons and multipeaked solitons. Flat-topped solitons link the defect solitons in a small index core and the symmetric kink pairs or surface wave pairs in a large index core. Their existence region shrinks with the growth of the gain-loss component of the $\mathcal{PT}$ lattice. Multipeaked solitons with a different number of peaks can be found when the index core is large. The peak amplitudes of the soliton modulus or intensity are of the same value. Linear stability analysis corroborated by direct propagation simulations reveals that both families of solitons are either completely stable (in lattices with weak gain and loss) or suffer a weak oscillatory instability (in lattices with strong gain and loss). Unstable solitons can propagate robustly for a very long propagation distance, even when the gain-loss coefficient is close to the $\mathcal{PT}$-symmetry-breaking point. This is in sharp contrast to the stability of solitons in single-site defected or regular $\mathcal{PT}$ lattices.

ACKNOWLEDGMENTS

This work is supported by the National Natural Science Foundation of China (Grant No. 11374268) and the Natural Science Foundation of Zhejiang Province, China (Grant No. LY13A040003).

[1] F. Lederer, G. I. Stegeman, D. N. Christodoulides, G. Assanto, M. Segev, and Y. Silberberg, Discrete solitons in optics, Phys. Rep. **463**, 1 (2008).
[2] Z. H. Musslimani, K. G. Makris, R. El-Ganainy, and D. N. Christodoulides, Optical solitons in PT periodic potentials, Phys. Rev. Lett. **100**, 030402 (2008).
[3] A. Guo, G. J. Salamo, D. Duchesne, R. Morandotti, M. Volatier-Ravat, V. Aimez, G. A. Siviloglou, and D. N. Christodoulides, Observation of PT-Symmetry breaking in complex optical potentials, Phys. Rev. Lett. **103**, 093902 (2009).
[4] C. E. Rüter, K. G. Makris, R. El-Ganainy, D. N. Christodoulides, M. Segev, and D. Kip, Observation of parity-time symmetry in optics, Nat. Phys. **6**, 192 (2010).
[5] C. M. Bender and S. Boettcher, Real spectra in Non-Hermitian Hamiltonians having PT symmetry, Phys. Rev. Lett. **80**, 5243 (1998).
[6] C. M. Bender, D. C. Brody, and H. F. Jones, Complex extension of quantum mechanics, Phys. Rev. Lett. **89**, 270401 (2002).
[7] K. G. Makris, R. El-Ganainy, D. N. Christodoulides, and Z. H. Musslimani, Beam dynamics in PT symmetric optical lattices, Phys. Rev. Lett. **100**, 103904 (2008).
[8] F. K. Abdullaev, Y. V. Kartashov, V. V. Konotop, and D. A. Zezyulin, Solitons in PT-symmetric nonlinear lattices, Phys. Rev. A **83**, 041805 (2011).
[9] D. A. Zezyulin, Y. V. Kartashov, and V. V. Konotop, Stability of solitons in PT-symmetric nonlinear potentials, Europhys. Lett. **96**, 64003 (2011).
[10] Y. He, X. Zhu, D. Mihalache, J. Liu, and Z. Chen, Lattice solitons in PT-symmetric mixed linear-nonlinear optical lattices, Phys. Rev. A **85**, 013831 (2012).
[11] K. Zhou, Z. Guo, J. Wang, and S. Liu, Defect modes in defective parity-time symmetric periodic complex potentials, Opt. Lett. **35**, 2928 (2010).
[12] H. Wang and J. Wang, Defect solitons in parity-time periodic potentials, Opt. Express **19**, 4030 (2011).
[13] S. Nixon, L. Ge, and J. Yang, Stability analysis for solitons in PT-symmetric optical lattices, Phys. Rev. A **85**, 023822 (2012).
[14] Z. Shi, X. Jiang, X. Zhu, and H. Li, Bright spatial solitons in defocusing Kerr media with PT-symmetric potentials, Phys. Rev. A **84**, 053855 (2011).
[15] Y. V. Kartashov, B. A. Malomed, and L. Torner, Unbreakable PT symmetry of solitons supported by inhomogeneous defocusing nonlinearity, Opt. Lett. **39**, 5641 (2014).
[16] C. Huang, F. Ye, Y. V. Kartashov, B. A. Malomed, and X. Chen, PT symmetry in optics beyond the paraxial approximation, Opt. Lett. **39**, 5443 (2014).
[17] J. Yang, Symmetry breaking of solitons in one-dimensional parity-time-symmetric optical potentials, Opt. Lett. **39**, 5547 (2014).
[18] J. Yang, Partially PT symmetric optical potentials with all-real spectra and soliton families in multidimensions, Opt. Lett. **39**, 1133 (2014).
[19] C. P. Jisha, L. Devassy, A. Alberucci, and V. C. Kuriakose, Influence of the imaginary component of the photonic potential on the properties of solitons in $\mathcal{PT}$-symmetric systems, Phys. Rev. A **90**, 043855 (2014).
[20] C. P. Jisha, A. Alberucci, V. A. Brazhnyi, and G. Assanto, Nonlocal gap solitons in $\mathcal{PT}$-symmetric periodic potentials with defocusing nonlinearity, Phys. Rev. A **89**, 013812 (2014).
[21] P. S. J. Russell, Photonic crystal fibers, Science **299**, 358 (2003).
[22] J. C. Knight and D. V. Skryabin, Nonlinear waveguide optics and photonic crystal fibers, Opt. Express **15**, 15365 (2007).
[23] B. Freedman, G. Bartal, M. Segev, R. Lifshitz, D. N. Christodoulides, and J. W. Fleischer, Wave and defect dynamics in nonlinear photonic quasicrystals, Nature (London) **440**, 1166 (2006).
[24] J. Yang and Z. Chen, Defect solitons in photonic lattices, Phys. Rev. E **73**, 026609 (2006).

[25] F. Ye, Y. V. Kartashov, V. A. Vysloukh, and L. Torner, Bragg guiding of domainlike nonlinear modes and kink arrays in lower-index core structures, Opt. Lett. **33**, 1288 (2008).

[26] S. Zhong, C. Huang, C. Li, and L. Dong, Symmetric and antisymmetric solitons in finite lattices, Opt. Express **19**, 17179 (2011).

[27] L. Dong and F. Ye, Shaping solitons by lattice defects, Phys. Rev. A **82**, 053829 (2010).

[28] S. Hu, X. Ma, D. Lu, Y. Zheng, and W. Hu, Defect solitons in parity-time-symmetric optical lattices with nonlocal nonlinearity, Phys. Rev. A **85**, 043826 (2012).

[29] C. Li, C. Huang, H. Liu, and L. Dong, Multipeaked gap solitons in PT-symmetric optical lattices, Opt. Lett. **37**, 4543 (2012).

[30] G. P. Agrawal, *Nonlinear Fiber Optics*, 4th ed. (Academic Press, Boston, 2007).

[31] J. Yang, *Nonlinear Waves in Integrable and Nonintegrable Systems* (SIAM, Philadelphia, 2010).

[32] Y. V. Kartashov, V. A. Vysloukh, and L. Torner, Surface gap solitons, Phys. Rev. Lett. **96**, 073901 (2006).

[33] H. S. Sözüer, J. W. Haus, and R. Inguva, Photonic bands: Convergence problems with the plane-wave method, Phys. Rev. B **45**, 13962 (1992).

[34] J. Yang and T. I. Lakoba, Universally-convergent squared-operator iteration methods for solitary waves in general nonlinear wave equations, Stud. Appl. Math. **118**, 153 (2007).

[35] Y. V. Kartashov, V. A. Vysloukh, and L. Torner, Surface lattice kink solitons, Opt. Express **14**, 12365 (2006).

[36] J. Wang, J. Yang, T. J. Alexander, and Y. S. Kivshar, Truncated-Bloch-wave solitons in optical lattices, Phys. Rev. A **79**, 043610 (2009).

[37] C. Li, H. Liu, and L. Dong, Multi-stable solitons in PT-symmetric optical lattices, Opt. Express **20**, 16823 (2012).